Structural and Metamorphic Evolution of the Robertson River Metamorphics

with Pressure-Temperature-Deformation-Time (P-T-D-t) Path

VOLUME II

Thesis submitted by

Mustafa Cihan (Bsc, Msc, at METU in Turkey)

In October 2004

For the degree of Doctor of Philosophy

in the School of Earth Sciences, James Cook University

Townsville, Australia

Contents of Volume II

List of Figures and Tables

Section A

Section B

Section C

Section D

SECTION -A-

THE DRAWBACKS OF SECTIONING ROCKS RELATIVE TO FABRIC ORIENTATIONS IN THE MATRIX: A CASE STUDY FROM THE ROBERTSON RIVER METAMORPHICS (NORTHERN QUEENSLAND, AUSTRALIA)

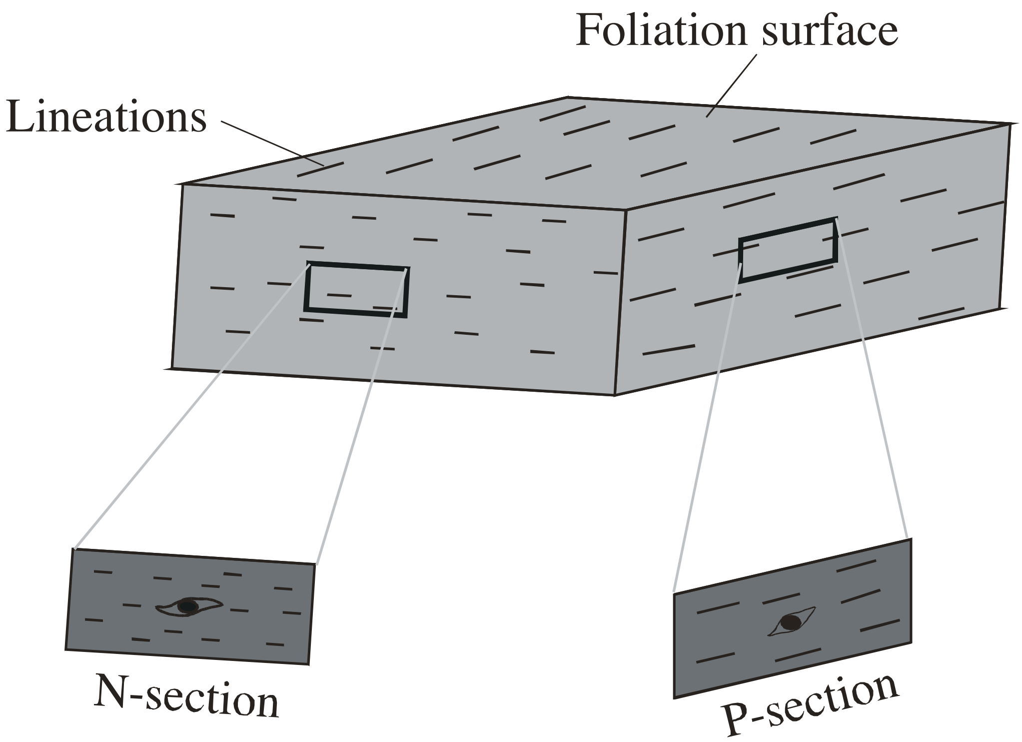

Figure 1. Sketch showing a P section (perpendicular to foliation plane and parallel to lineation) and an N section (perpendicular to foliation and lineation).

7923000 0

THIS IMAGE HAS BEEN REMOVED DUE TO COPYRIGHT RESTRICTIONS

7908000
0760000

Figure 2. Location map showing major regional geological features and the area in which detailed work done outlined by a box.

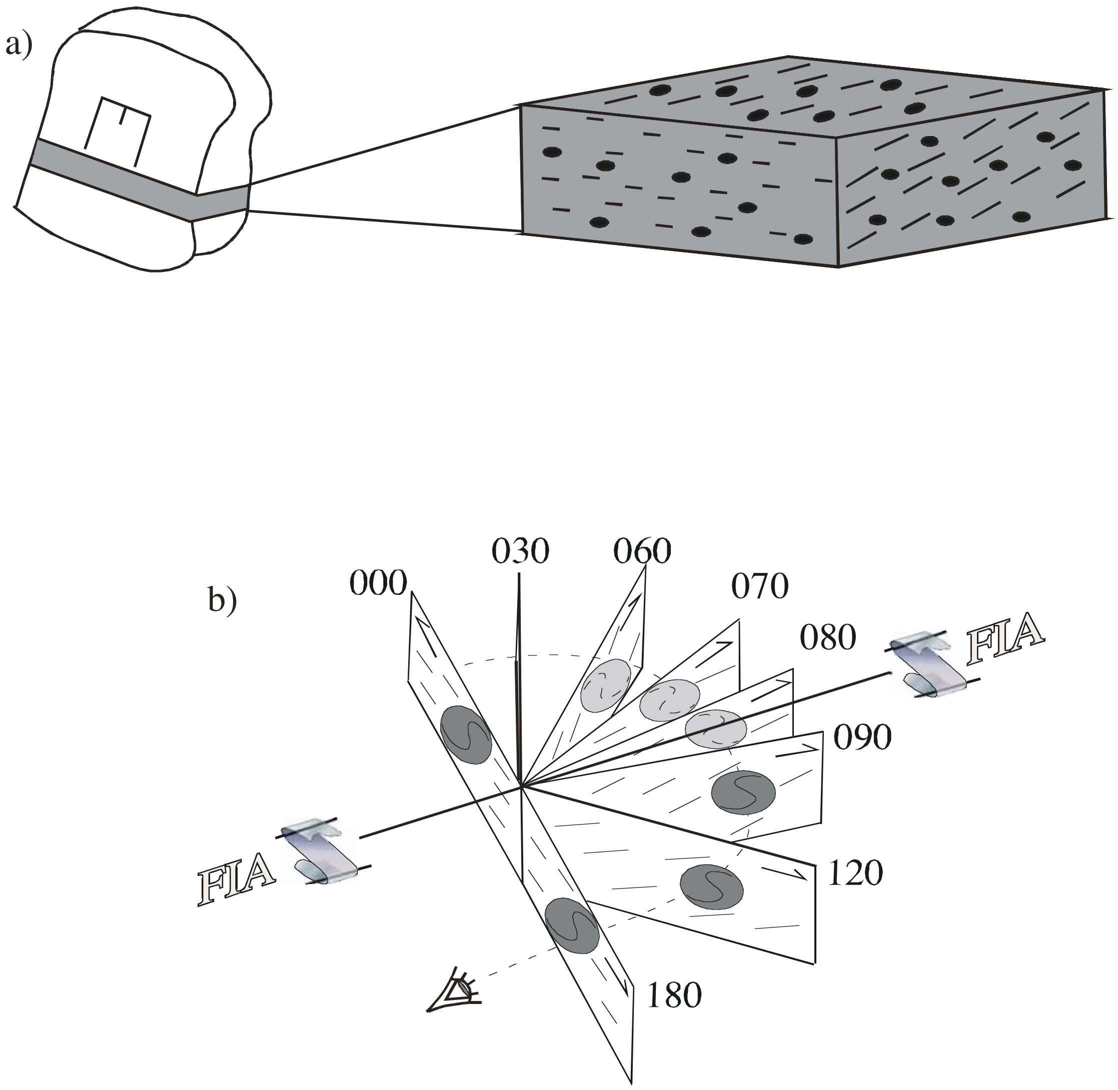

Figure 3. Sketches of the oriented rock sample marked and cut into a horizontal slab (a) and multiple-vertical thin sections (b). FIA is the foliation intersection/inflection axis preserved within porphyroblasts.

Figure 4. Photographs and line diagrams (a-g) of garnet porphyroblasts taken from vertical thin sections in different orientations around compass. Shaded areas at the core of the porphyroblasts in c, d, e and f represents early growth of these and can only be observed in these orientations.

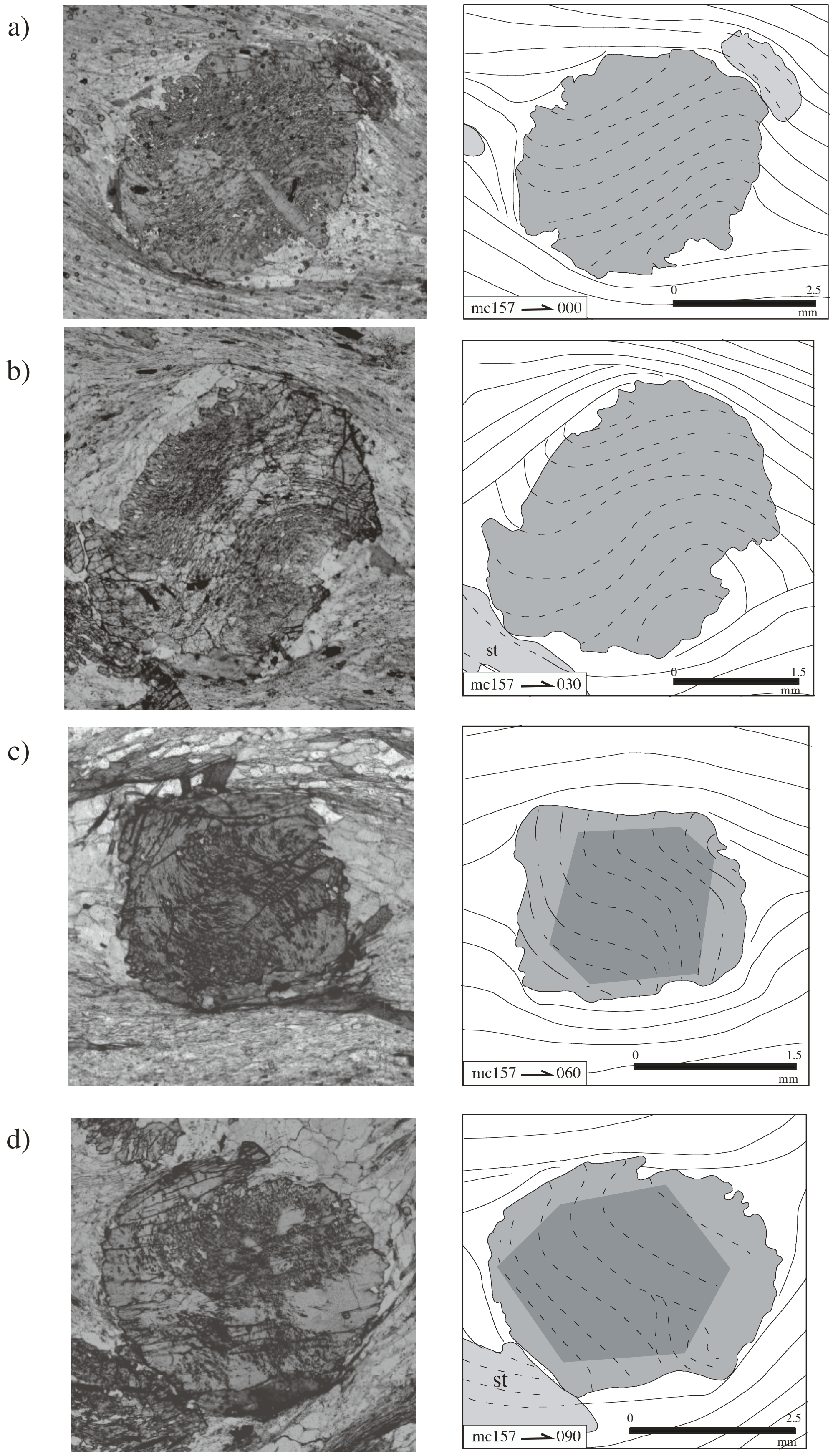
a)
0
2.5
mm
mc157 000
b)
st
0
1.5
mm
mc157 030
c)
0
1.5
mm
mc157 060
d)
st
0
2.5
mm
mc157 090

e)

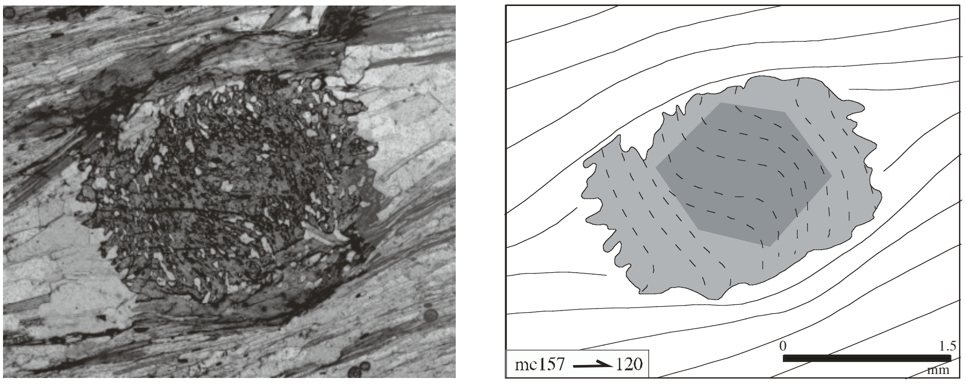
mc157 → 120
0
1.5
mm

f)

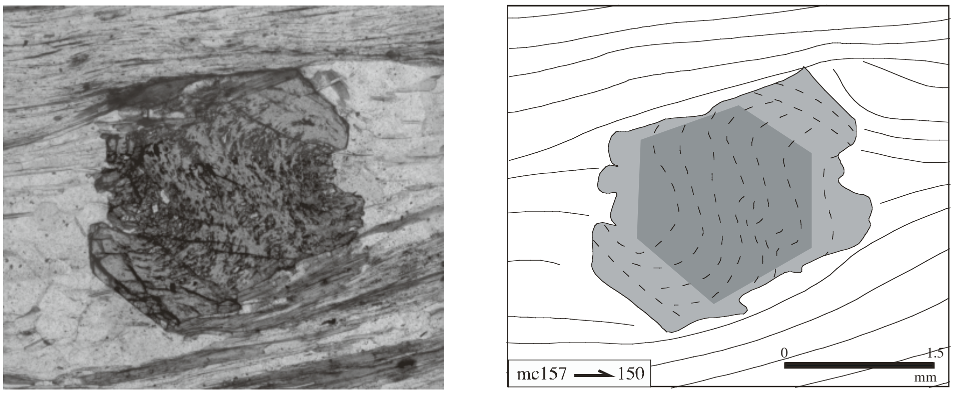
mc157 → 150
0
1.5
mm

g)

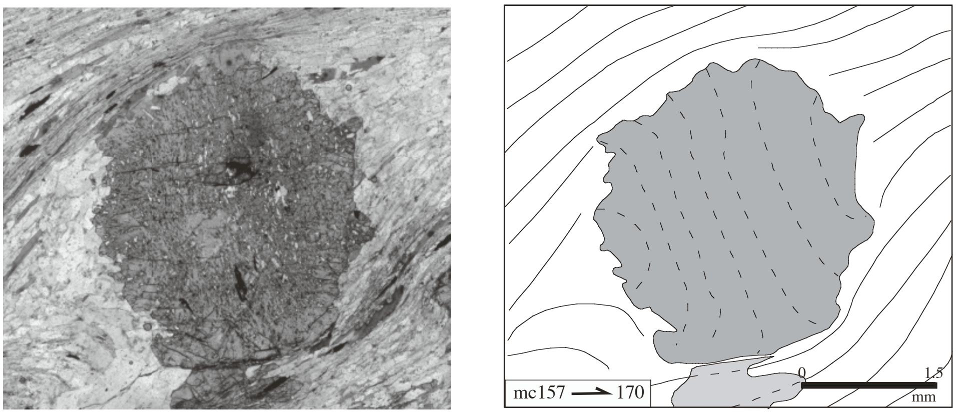
mc157 → 170
0
1.5
mm

h)

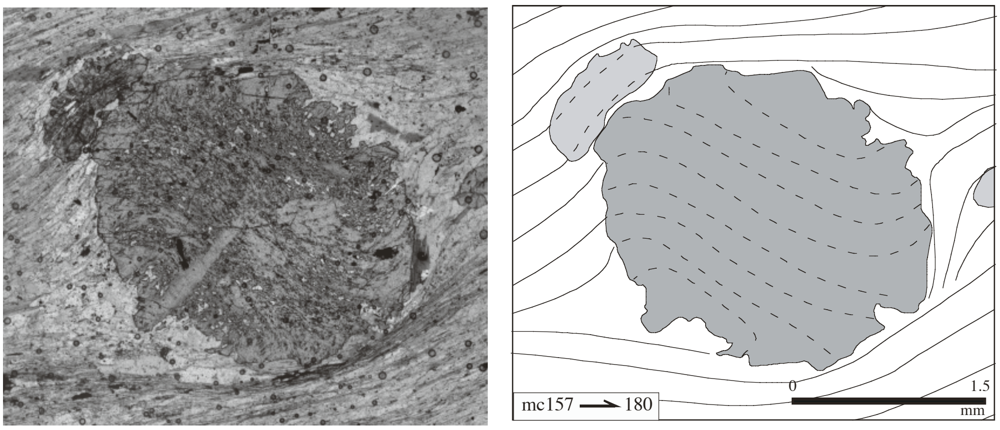
mc157 → 180
0
1.5
mm

Sample Number	Garnet		Staurolite	
	Core	Rim	Core	Rim
mc1.1	105		175	
mc1.2	105			
mc103	35			
mc105	85	175		
mc108	95			
mc110	155			
mc12	85		175	
mc121	35			
mc13	175			
mc130	55		175	
mc132A	85		15	
mc132B	65		175	
mc133	175		45	
mc134	145		25	
mc135	125			
mc137	85		175	
mc14.1	25		175	
mc14.2	95		15	
mc140	65		85	
mc15	5			
mc151	85			
mc152	65	85	175	35
mc153	95			
mc154	55			
mc157	175		175	45
mc158	175		45	
mc159	15			
mc160	75		45	
mc17	95	175	15	
mc2	105			
mc20			85	
mc21			85	
mc22			175	
mc23	95			
mc24	105			
mc24.1	85	175		
mc25	105			
mc26	175			
mc27	175			
mc28	175			
mc3	125			
mc30	85		45	
mc31	155		175	
mc32	55		45	
mc33	115			
mc34	25			
mc35.1	35		35	
mc35.2	90			
mc36	65	85		
mc37	85	175	45	
mc38	55			
mc39	65	85	25	
mc49	65	175		
mc5	55	15	175	45
mc55	85		15	45
mc58	65			
mc6	95		35	
mc65	65			
mc66	85			
mc68	105		175	
mc7	15		45	
mc71	85			
mc8	175		175	
mc81	175	15	45	
mc84	65		45	
mc87	55			
mc9	175		175	

Table 1. A list of FIA measurements for each sample from core and rim of garnet and staurolite porphyroblasts.

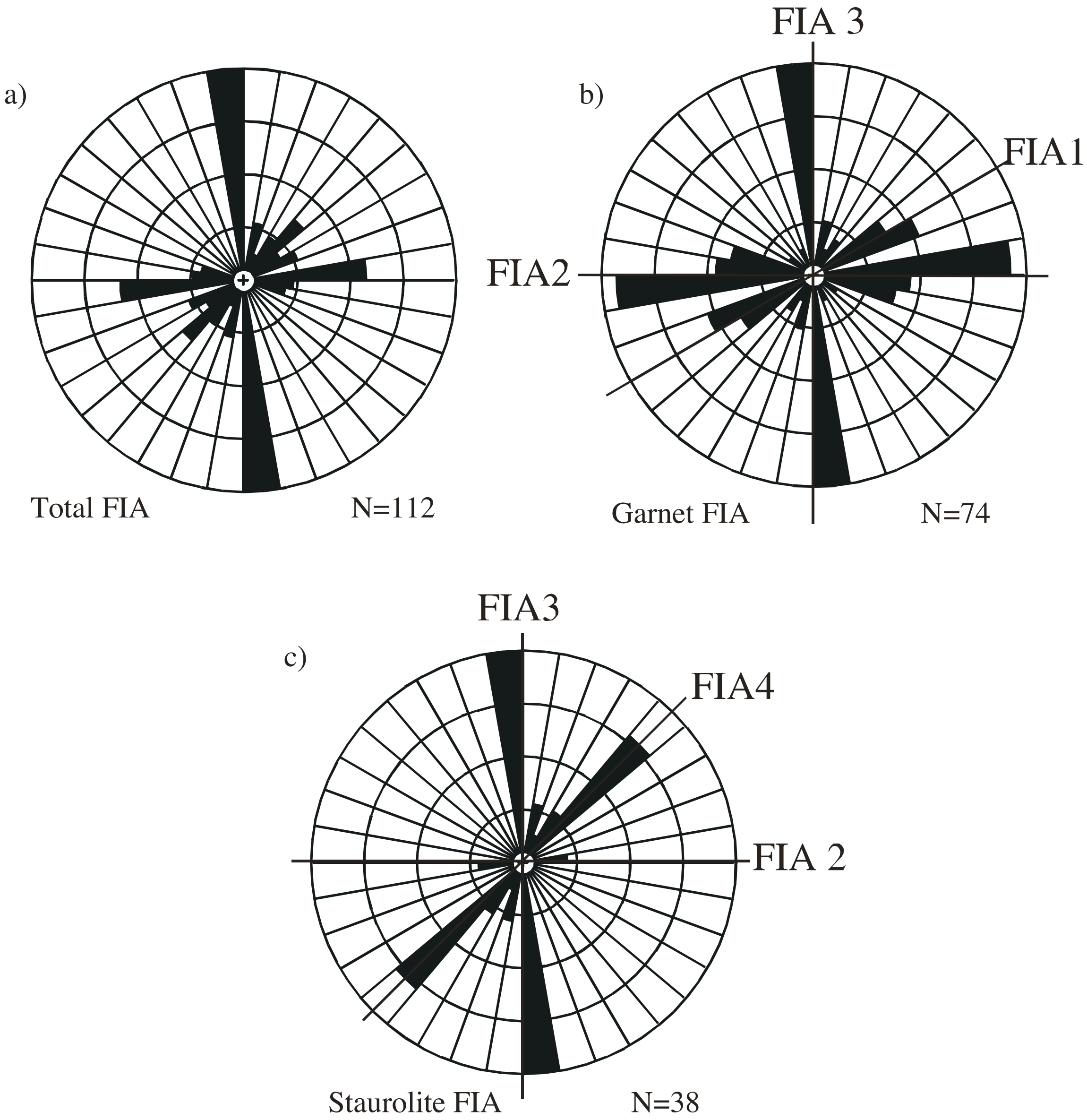

Figure 5. Rose diagrams of total FIA trends (a), garnet FIAs (b) and staurolite FIAs (c).

Table 2. Test of null hypothesis that the FIAs measured in rock samples are a sample of a random population using Watson`s U^2 test statistic for grouped data. The result (0.526) exceeds the U^2 value (0.268) at the 0.01 level of significance, suggesting the null hypothesis can be rejected and that the population is not random (FIA trends were initially doubled to convert them from axial to directional data; modulo 360°).

10° groupings	*j* group	n_j	S_j (np_j= 3.642) (p=10/360)	$(S_j)^2$	$U^2_{grouped}$
360°-009°	1	0	-2.889	8.346	
010°-019°	2	1	-4.778	22.827	
020°	3	0	-7.667	58.778	
030°	4	8	-2.556	6.531	
040°	5	0	-5.444	29.642	
050°	6	4	-4.333	18.778	
060°	7	0	-7.222	52.160	
070°	8	7	-3.111	9.679	
080°	9	0	-6.000	36.000	
090°	10	11	2.111	4.457	
100°	11	0	-0.778	0.605	
110°	12	6	2.333	5.444	
120°	13	0	-0.556	0.309	
130°	14	8	4.556	20.753	
140°	15	0	1.667	2.778	
150°	16	1	-0.222	0.049	
160°	17	0	-3.111	9.679	
170°	18	17	11.000	121.000	
180°	19	1	9.111	83.012	
190°	20	6	12.222	149.383	
200°	21	0	9.333	87.111	
210°	22	6	12.444	154.864	
220°	23	0	9.556	91.309	
230°	24	1	7.667	58.778	
240°	25	0	4.778	22.827	
250°	26	2	3.889	15.123	
260°	27	0	1.000	1.000	
270°	28	0	-1.889	3.568	
280°	29	0	-4.778	22.827	
290°	30	1	-6.667	44.444	
300°	31	0	-9.556	91.309	
310°	32	2	-10.444	109.086	
320°	33	0	-13.333	177.778	
330°	34	1	-15.222	231.716	
340°	35	0	-18.111	328.012	
350°-359°	36	29	8.000	64.000	
	TOTAL	112	-29.000	2143.963	0.526

3 groups

actual	garnet	staurolite
127°-020°	24	18
021°-50°	5	17
051°-126°	45	3
	74	38
$X^2 =$	55.2003	
d.f. = 2	$X^2_{0.05} = 5.99$	
P =	6.2228E-12	

using 5 rather than 3 groups

actual	garnet	staurolite
180°-030°	7	6
031°-070°	17	15
071°-120°	29	3
121°-160°	5	0
161°-179°	16	14
	74	38
$X^2 =$	37.2494	
d.f. = 4	$X^2_{0.05} = 9.49$	
P =	1.6003E-07	

Table 3. X^2 test of independence of the null hypothesis that the distribution of the variables (FIA trends) is from the same population. Test results are assessed at the 0.05 level of significance. The outcome of the test suggests that garnet and staurolite FIAs differ significantly from each other.

Figure 6. Compositional maps (Mg, Ca, Mn, Fe) of a garnet porphyroblast from sample mc37.

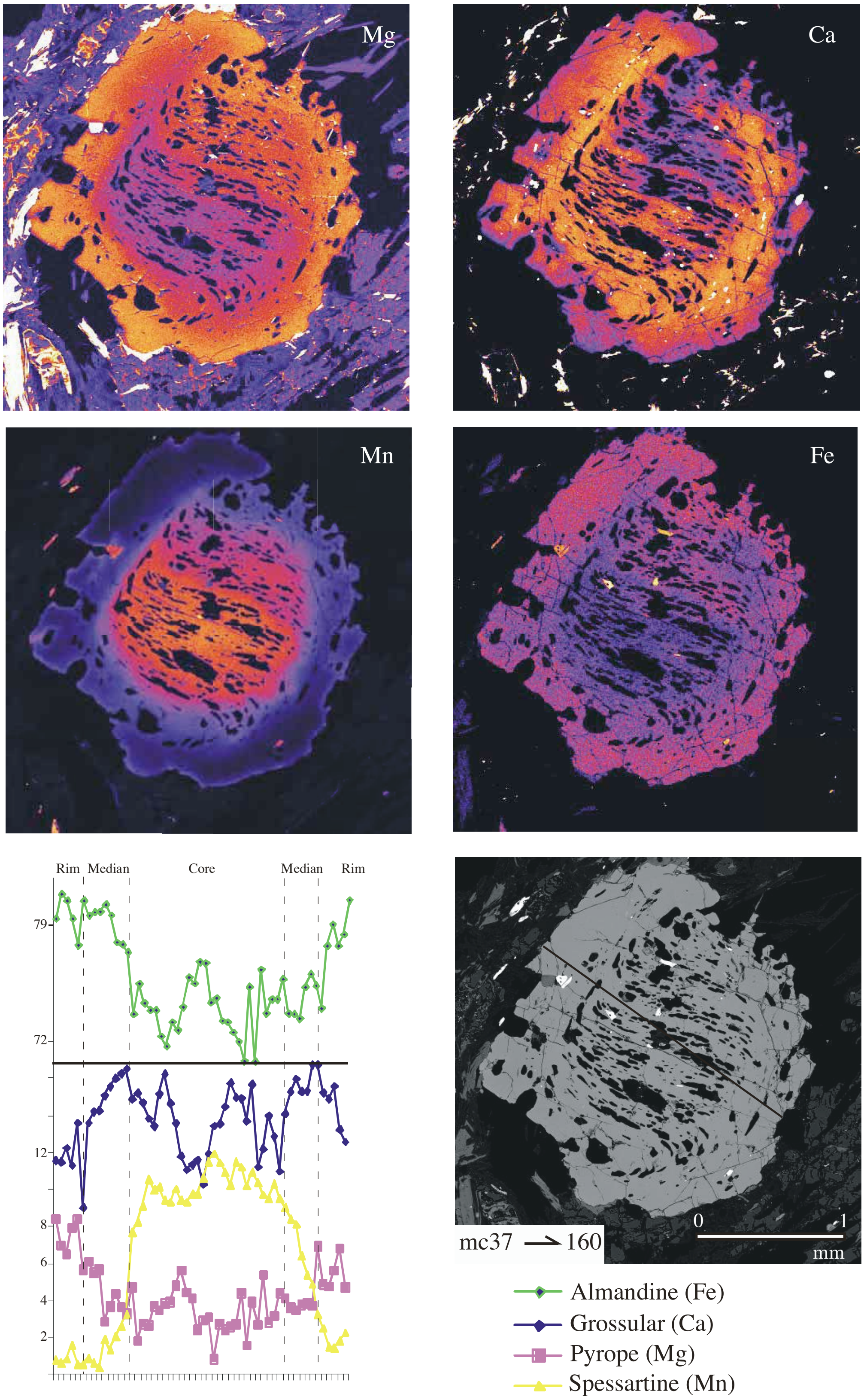
Mg
Ca
Mn
Fe
Rim
Median
Core
Median
Rim
79
72
12
8
6
4
2
0
1
mm
mc37
160
Almandine (Fe)
Grossular (Ca)
Pyrope (Mg)
Spessartine (Mn)

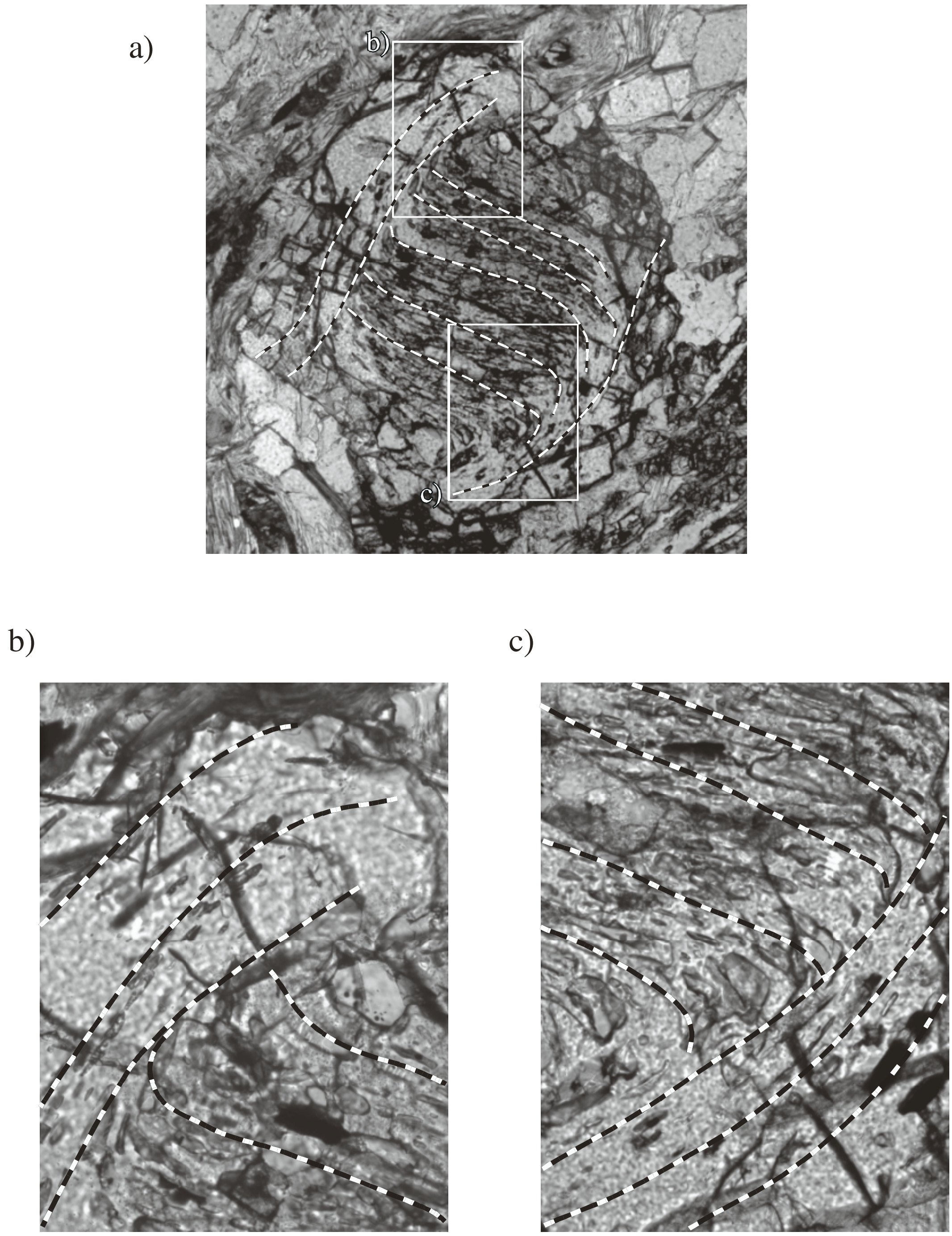

Figure 7. Photograph of the same garnet porphyroblast in Fig. 6 containing sigmoidal type inclusion trails (a). Close-up views show flat lying inclusions truncated sharply by the rim inclusions (b, c). Boxes A and B show the positions of the close-up views.

a)

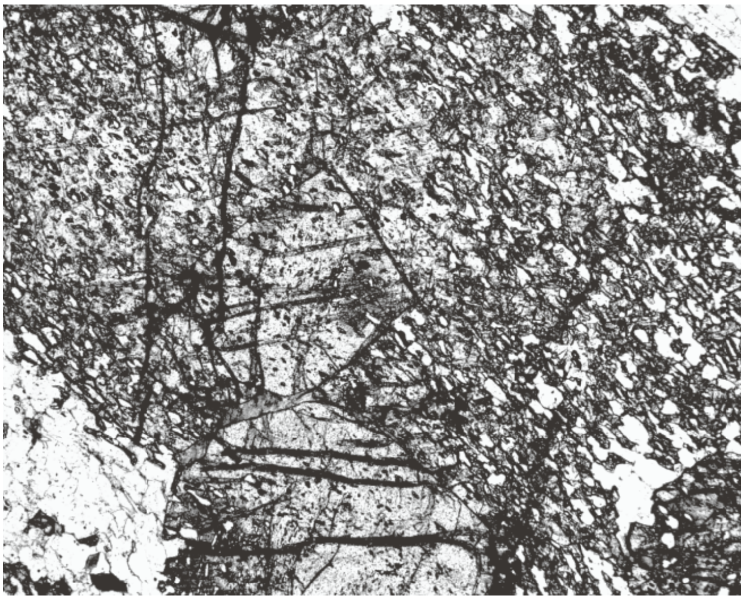

b)

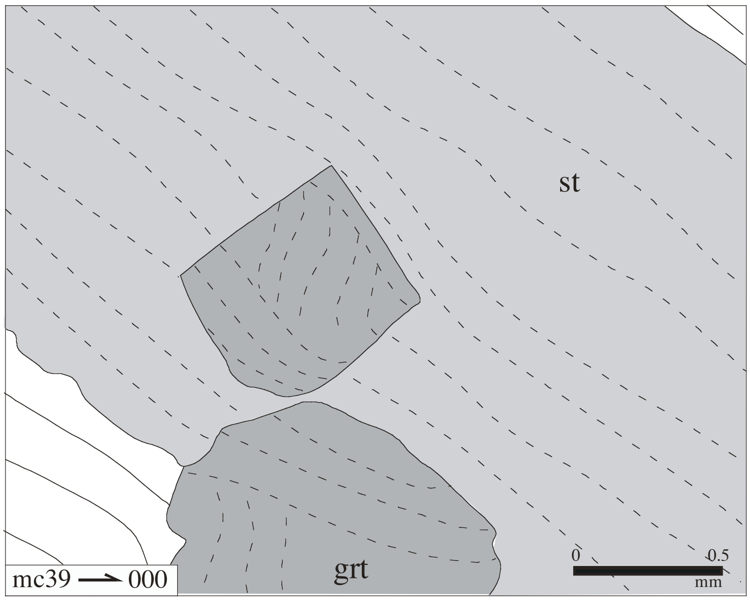

Figure 8. Photograph and a line diagram showing a staurolite (st) porphyroblast containing two garnet (grt) porphyroblasts. The inclusion trails within staurolite porphyroblasts are continuous with the matrix and rim inclusions, whereas the ones in the core of garnet porphyroblasts are truncated.

Figure 9. Photographs of garnet porphyroblasts from N (a) and P (b) sections. In both sections the inclusion trails are continuous into the strain shadows and superficially appear to be continuous with the matrix foliation.

a)

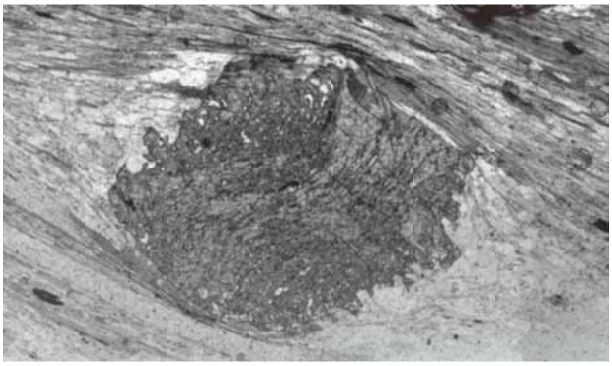

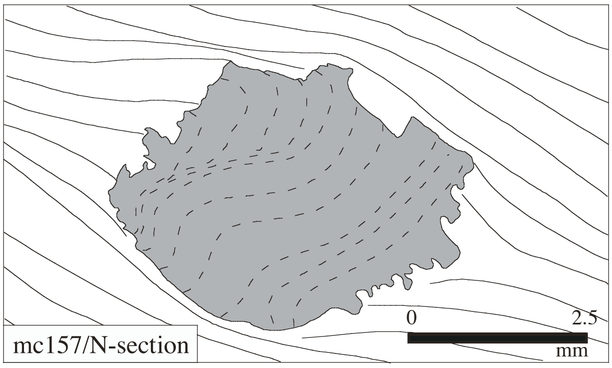

b)

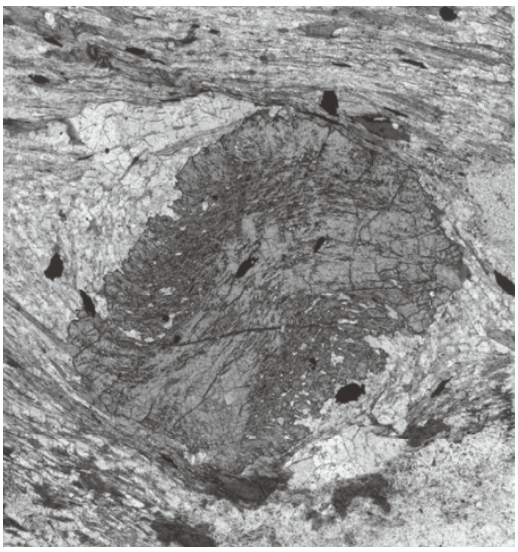

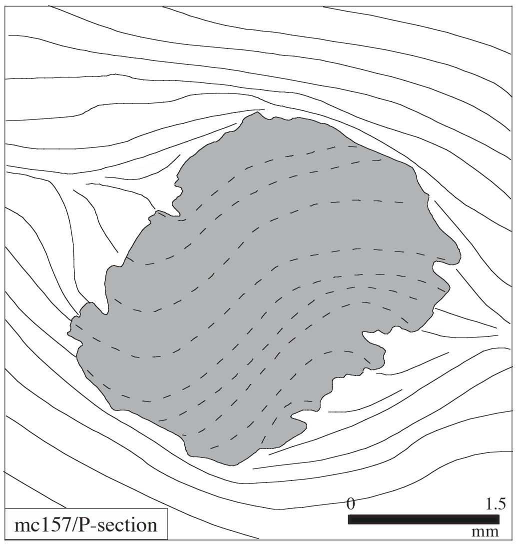

Figure 10. Photograph of a staurolite porphyroblast overgrowing differentiated crenulation cleavage, whose trails are continuous with the matrix foliation.

a)

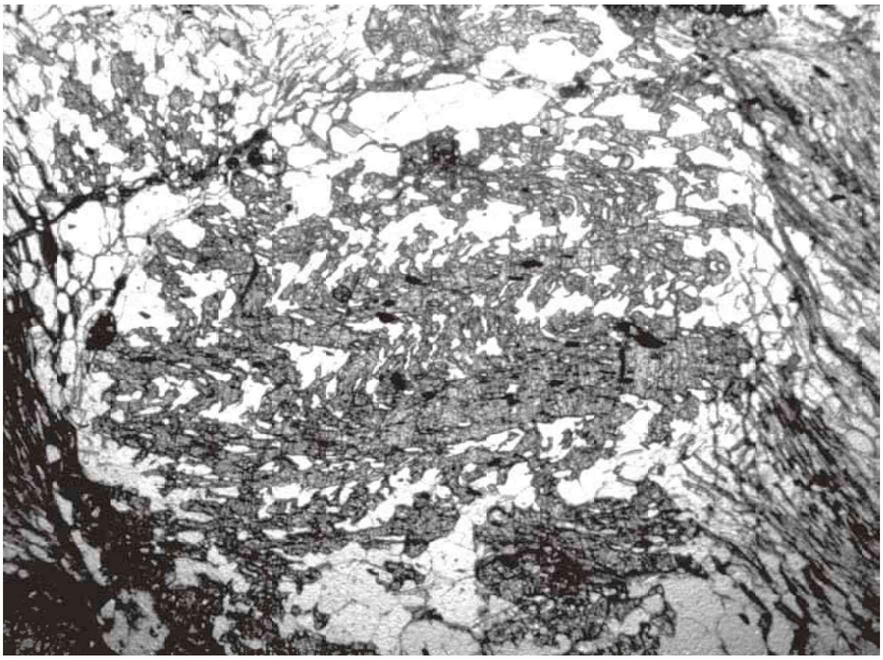

b)

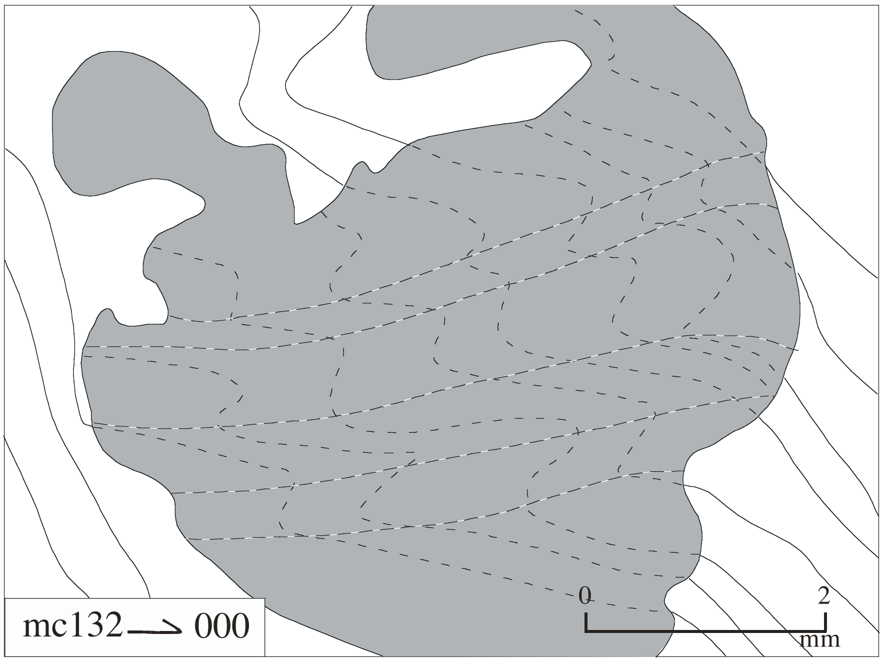

Figure 11. Photograph and a line diagram showing two staurolite porphyroblasts, which have grown adjacent to one another with sigmoidal type inclusions, which are continuous with the matrix (a). The porphyroblasts preserve between them a steep crenulation cleavage (thick vertical dash lines on a line diagram), in which clockwise (sinistral) shear sense was acting (b). This steep foliation has been destroyed in the matrix by reactivation. The shear senses, operating during development of the crenulation cleavage and during reactivation are shown with barbed arrows.

a)

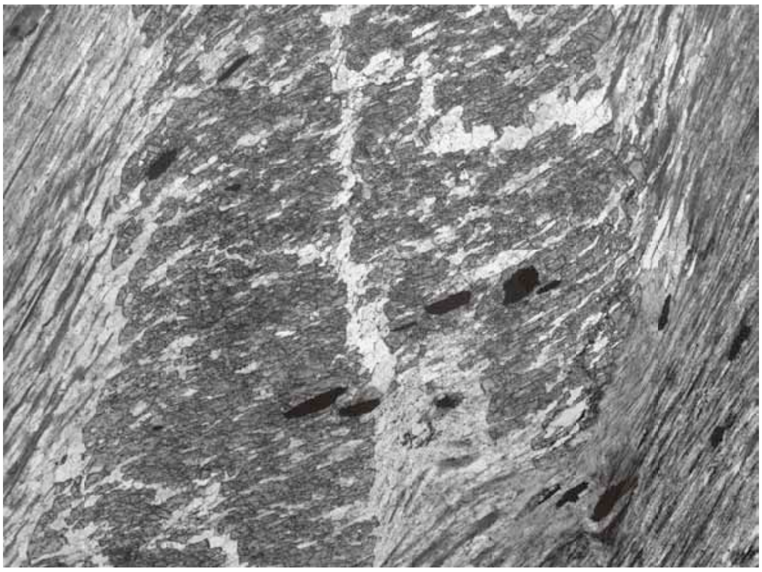

b)

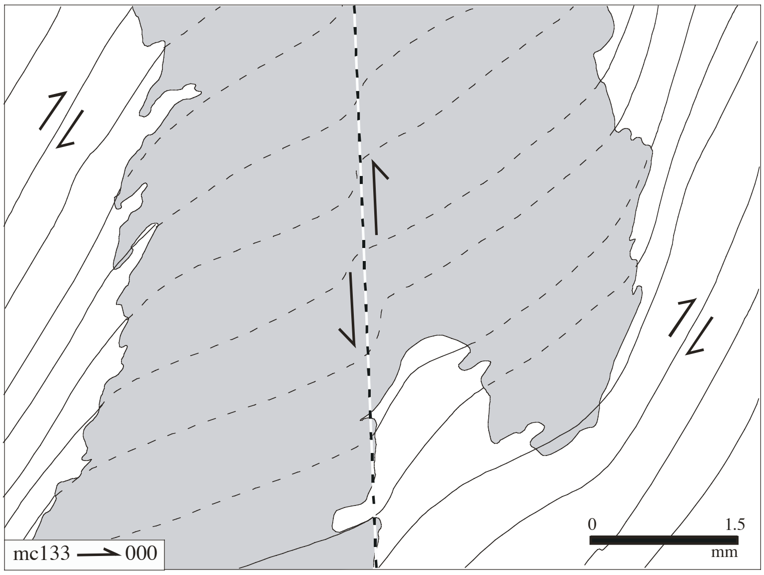

Figure 12. Steorenet projections of the FIA1-4 showing the effect of rotation around the mean trend of the next FIA in the succession. In (a), rotation effect of FIA1 around E-W axis; FIA2, shown with darker shaded area. FIA1 trend would lie in that shaded area in any orientation with gentle plunges, if they were rotated around FIA2. Apart from that the rotation of both FIA1 and FIA2 are shown around FIA3 as well. They would lie in the range shown by shaded areas in northern and southern quadrants, if they were again rotated. In (b) the rotation of FIA1-3 is shown around FIA4 axis. If they were rotated, FIA1 would lie in darker shaded area, and FIA2 and FIA3 would lie in any orientation in NE-SW quadrants.

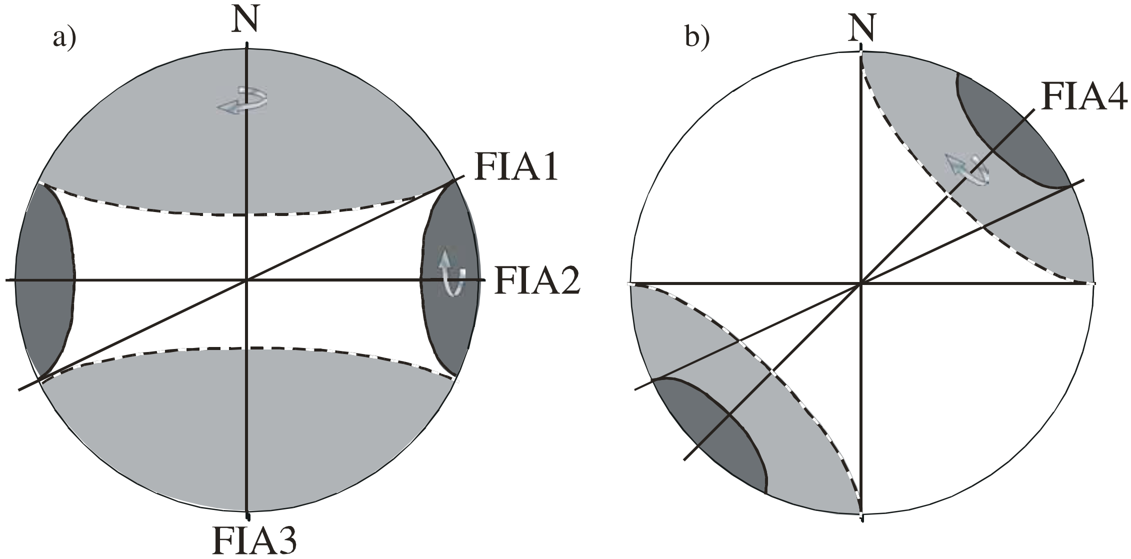
a)
N
FIA1
FIA2
FIA3
b)
N
FIA4

Figure 13. Simplified sketch showing the growth of a porphyroblast. In (a), deformation partitions into progressive shearing and shortening domains as represented by crenulation cleavage and hinge of a crenulation respectively. The first porphyroblast growth occurs on a hinge of crenulation cleavage (progressive shortening domain) at the beginning of D_2 event. In (b), if reactivation occurs, S_1 is decrenulated and rotated towards compositional layering in the matrix (S_{1r}). In (c), deformation repartitions during D_3, and the growth of rim occurs. The earlier foliation, S_2 or S_{1r} in the case of reactivation, which intensified in the matrix during the late stages of D_2, is trapped as inclusion trails.

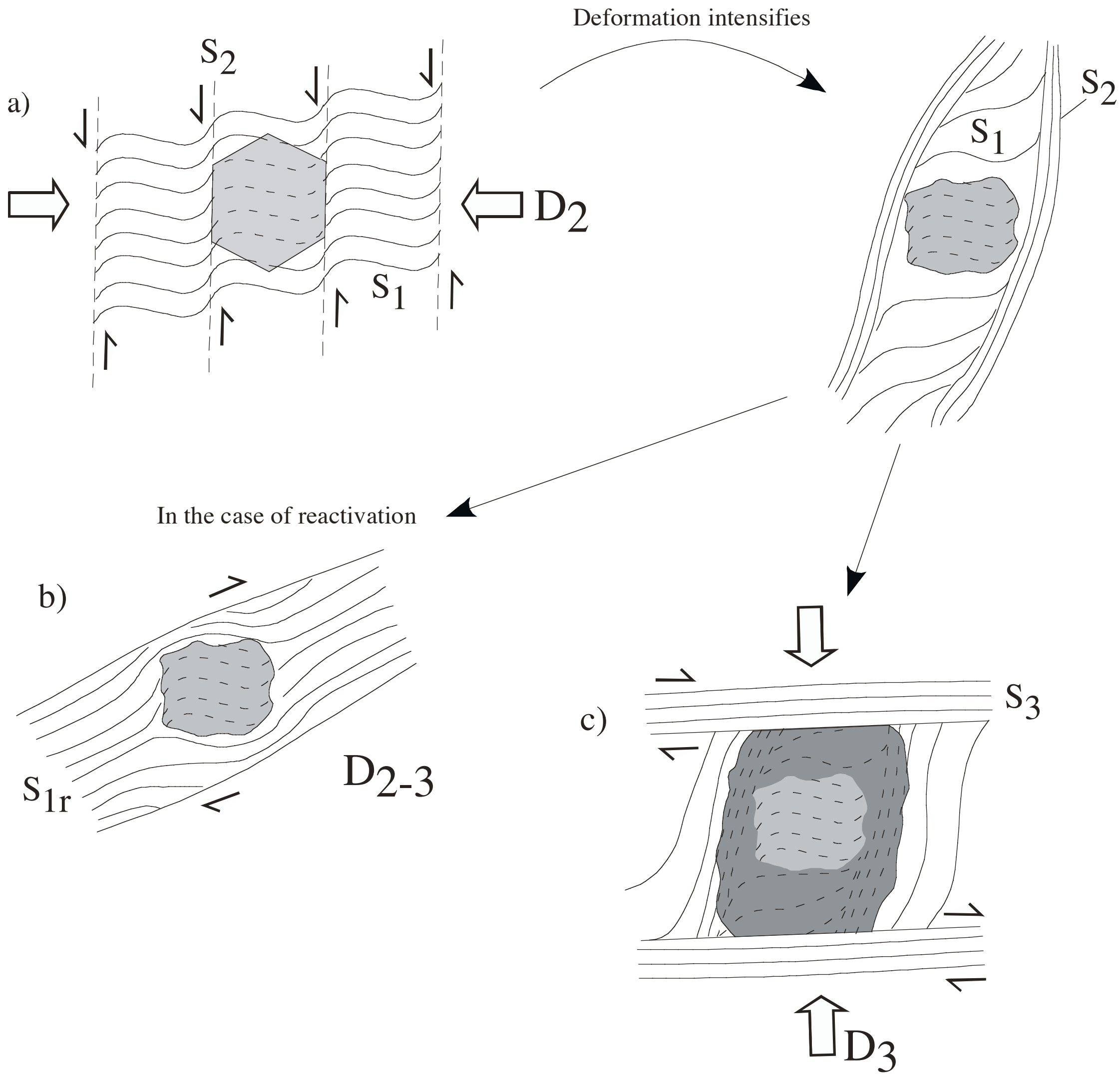
Deformation intensifies
a)
S_2
D_2
S_1
S_2
S_1
In the case of reactivation
b)
S_{1r}
D_{2-3}
c)
S_3
D_3

Figure 14. Sketches showing the effect of reactivation (modified from Bell et al., 1986). In (a), anastomosing S_2 foliations formed with synthetic sinistral shear sense parallel to the axial plane of newly developing fold. The inset shows the strain field diagram in which deformation partitions into progressive shearing and shortening domains. In (b), as the deformations continues the fold tightens more and bedding ($S_{0,1}$) reactivates. During this stage, synthetic shear sense acting on S_2 switches to antithetic shear sense along the bedding in a reactivated area in which S_2 is destroyed, and the earlier foliation, S_1, decrenulates and rotates towards the bedding.

a)

THE IMAGES ON THIS PAGE HAVE BEEN REMOVED DUE TO COPYRIGHT RESTRICTIONS

b)

Figure 15. 3D sketch of a porphyroblast having inclusions that are oblique to and truncated, by the matrix foliation planes, with the detailed view along A-B orientation showing the relationship of S1, S2 and S3 (a). P and N sections cut from 3D block sketch show the continuation of the inclusion trails with matrix. In these sections, inclusions trapped in the strain shadows, especially in the N section, are misinterpreted as S1, but in fact it is S2 (b). However, in multiple-vertical thin sections in 120° and 150° orientations, inclusion trails are truncated by the matrix foliations. S1 is the earliest foliation trapped as inclusion in porphyroblast; S2 is the earlier matrix foliation; S3 is lately formed foliation; Barbed arrows show shear senses; A-B, C-D, E-F, G-H show the positions of sections; N is true north.

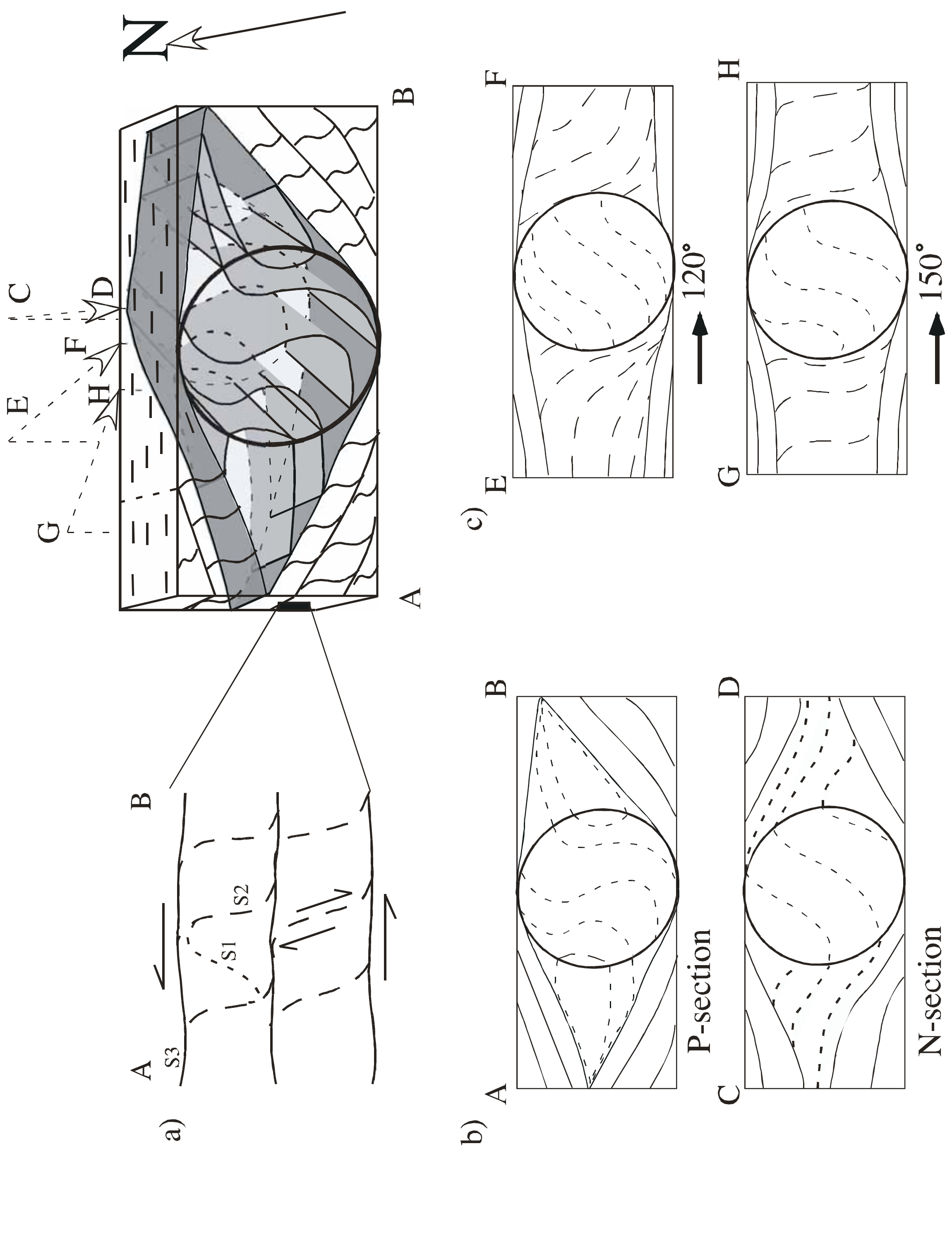
N
A
B
C
D
E
F
G
H
a)
S1
S2
S3
b)
P-section
N-section
c)
120°
150°